





CLINICAL ARTICLE

Cortical Endplate Bone Density Measured by Novel Phantomless Quantitative Computed Tomography May Predict Cage Subsidence more Conveniently and Accurately

Mingyuan Di, MD^{1,2}, Yuanzhi Weng, MSc^{3,4} , Guohua Wang, MD^{1,2}, Hanming Bian, MD^{1,2} , Huan Qi, PhD^{3,4}, Hongjin Wu, MD^{1,2}, Chao Chen, MD, PhD², Yiming Dou, MD², Zhi Wang, MD⁵, Xinlong Ma, MD² , Baoshan Xu, MD, PhD², Shan Zhu, MSc⁵, Weijia William Lu, PhD^{3,4}, Qiang Yang, MD, PhD² 

¹Graduate School, Tianjin Medical University, ²Department of Spine Surgery, Tianjin Hospital, Tianjin University and ⁵Tianjin Hospital of Tianjin University, Tianjin, ³Department of Orthopaedics and Traumatology, Li Ka Shing Faculty of Medicine, The University of Hong Kong, Pokfulam and ⁴Department of Orthopaedics and Traumatology, The University of Hong Kong-Shenzhen Hospital, Shenzhen, China

Objective: Previous studies have shown that bone mineral density (BMD) is a predictor of cage subsidence. Phantom-less quantitative computed tomography (PL-QCT) can measure volumetric bone mineral density (vBMD) of lumbar trabecular and cortical bone. The study of endplate vBMD (EP-vBMD) is important in predicting cage settlement after extreme lateral interbody fusion (XLIF). This study aimed to determine the risk factors for postoperative cage subsidence after XLIF, particularly focusing on the relationship between vBMD measured by automatic PL-QCT and cage subsidence.

Methods: Patients who underwent XLIF surgery from January 2018 to October 2020 with a minimum of 6 months of follow-up were retrospectively included. Cage subsidence was defined as >2 mm cage sinking on the adjacent endplate in follow-up imaging evaluation. Outcome measures were localized vBMDs included EP-vBMDs with different region of interest (ROI) heights measured by PL-QCT based on a customized muscle-fat algorithm. Shapiro–Wilk test, one-way ANOVA, Mann–Whitney test, Fisher exact test, univariable and multivariable logistic regression and receiver operating characteristic (ROC) curve analysis were executed in this study.

Results: One hundred and thirteen levels of 78 patients were included in the analysis. The mean age was 65 ± 7.9 years for 11 males and 67 females. Cage subsidence occurred on 45 (39.8%) surgical levels. There was no significant difference in demographics, fused levels, or preoperative radiographic parameters. 1.25-mm EP-vBMD (0.991 [0.985, 0.997], $p = 0.004$) and P-TB-vBMD (cage-positioned trabecular volumetric bone mineral density) (0.988 [0.977–0.999], $p = 0.026$) were cage-subsidence relevant according to univariate analysis. Low 1.25-mm EP-vBMD (0.992 [0.985, 0.999], $p = 0.029$) was an independent risk factor according to multifactorial analysis.

Conclusion: Preoperative low EP-vBMD was an independent risk factor for postoperative cage subsidence after XLIF. EP-vBMD measured by most cortex-occupied ROI may be the optimal vBMD parameter for cage subsidence prediction.

Key words: Cage subsidence; Endplate; Extreme lateral interbody fusion; Phantom-less quantitative computed tomography; Volumetric bone mineral density

Address for correspondence Qiang Yang, MD, PhD, Department of Spine Surgery, Tianjin Hospital, Tianjin University, No. 406 Jiefangnan Road, Hexi District, Tianjin 300211, China. Tel: +86 15102229608; Email: yangqiang1980@126.com Weijia William Lu, PhD, Department of Orthopaedics and Traumatology, Li Ka Shing Faculty of Medicine, The University of Hong Kong, Pokfulam, China. Tel: +852 87381980; Email: wlu@hku.hk.
Mingyuan Di, Yuanzhi Weng and Guohua Wang These authors contribute equally to this work.

Received 23 February 2023; accepted 20 July 2023



Introduction

Extreme lateral interbody fusion (XLIF) is a minimally invasive spinal surgical approach that avoids vascular injury in anterior lumbar interbody fusion (ALIF) through psoas major muscle entry. In comparison with transforaminal lumbar interbody fusion (TLIF) and posterior lumbar interbody fusion (PLIF), it also causes less damage to the paravertebral muscles.^{1,2} However, postoperative cage subsidence remains a risk factor that cannot be overlooked.³ Even in the case of XLIF which utilizes a larger cage with a better anti-subsidence design, the reported subsidence rate reaches approximately 20%.⁴ Cage subsidence causes changes in lumbar spinal alignment, leading to pain recurrence, failure of indirect decompression, and poor recovery of lumbar lordosis. Other problems of cage subsidence include segmental instability, fusion failure, and malformed bony fusion in inappropriate positions, potentially causing poorer functional recovery.⁵

Decreased bone mineral density (BMD) is a significant risk factor for cage migration and subsidence.^{6,7} Dual X-ray absorptiometry (DXA) is the gold standard for measuring BMD.⁸ However, only the whole spine can be examined by DXA and the average L1 to L4 bone quality can be characterized by areal BMD (aBMD) or T/Z-score.⁹ In cases of patients with osteophytes, cortical bone thickening, and aortic stenosis, DXA is inaccurate and unreliable. Formal studies have indicated that DXA results cannot reflect actual localized low bone mineral density within the vertebral body due to bone metabolism heterogeneity.¹⁰ Furthermore, DXA cannot measure localized BMD due to its instrumental principle, thus limiting its application.

Recently, many studies have applied quantitative computed tomography (QCT) for volumetric bone mineral density (vBMD) assessment. QCT is a technique for measuring vBMD in the human skeleton based on multi-row spiral CT scans with or without external calibration phantom. QCT has many advantages over DXA, including vBMD measurement, less susceptibility to degenerative spinal structures, and greater sensitivity to bone mass changes.^{11,12} The average L1-L2 trabecular vBMD (QCT-BMD) is used for osteoporosis screening.¹³ Automatic phantom-less QCT (PL-QCT) has excellent potential in measuring BMD due to its high accuracy and it can reduce radiation exposure and clinical costs by automatically circling regions of interest (ROIs) of fat and muscle for calibration.¹⁴

Previous studies have shown that endplate vBMD (EP-vBMD) measured by QCT with a 5 mm height ROI can be related to the cage subsidence of XLIF better compared to that of cancellous vBMD.^{15,16} Similar studies on oblique lumbar interbody fusion (OLIF) also indicate that endplate injury is a vital risk factor of cage subsidence.¹⁷ However, the osseous endplate thickness range is 0.35–1.03 mm, implying that the 5 mm height mainly comprises the trabecular bone.^{18–21} Considering the concave and irregular features of the endplate, a 1.25 mm height ROI for EP-vBMD measurement was included in this study. Trabecular vBMD (TB-vBMD) was also measured in adjacent vertebrae. Aims of this study were:

1. to confirm the optimal risk factors of cage subsidence in XLIF patients;
2. to confirm cage subsidence relevance degrees of vBMD measured on different regions; and
3. to determine the localized vBMD which most strongly correlated with cage subsidence.

We hypothesized that cage subsidence in XLIF may be most strongly correlated with most-cortex occupied endplate vBMD.

Methods

Automatically Calibrated PL-QCT Technique

The PL-QCT system (Bones QCT, Bones Technology Limited, Hong Kong, China) utilizes the subcutaneous fat and paraspinal muscle as the internal references and their coordinate ROIs were automatically placed for BMD calibration, thus improving vBMD measurement precision. The workflow of the automatic calibration technique has been reported in formal publications.¹⁴ The following are the steps included:

1. muscle and fat tissue segmentation through a HU range (*Muscle*: 20 ~ 80HU, *Fat*: -50 ~ -150HU) on calibration axial CT slice (Fig. 1);
2. a convolution map was constructed based on a kernel pyramid for better tissue boundaries robustness; and
3. finally, the optimal muscle and fat ROIs were automatically placed for calibration based on a priority algorithm, ensuring that calibrated ROIs were placed in locations closer to the vertebrae position provided by the user.

After automatic calibration, bone ROI could be modified further for localized vBMD measurement.

Patient Population

This study was approved by the Ethics Review Committee of Tianjin Hospital (IRB number: 2022 Medical Ethics Approval No.093). China. We reviewed the radiographic data of consecutive patients who underwent XLIF with posterior fixation from January 2018 to October 2020. The inclusion criteria were: (i) age greater than 45 years; (ii) patients have undergone XLIF surgery based on the Chinese XLIF diagnosis and treatment guide, preoperative diagnosis including lumbar spinal stenosis, lumbar foraminal stenosis, and degenerative scoliosis; (iii) CT scan was performed within one month before surgery; (iv) CT spatial resolution was 0.6 mm for x, y, and z directions; and (v) good radiographic imaging quality so that cage subsidence could be observed and over minimum 6 months follow up; The exclusion criteria were: (i) patients had vertebral fractures, tumors, tuberculosis, or infectious diseases; (ii) patients had medications related to bone metabolism; and (iii) intraoperative patients had damage to the endplate.

Surgical Procedures

Patients were in the lateral decubitus position and the target intervertebral space was supported by a cushion. Preoperative C-arm fluoroscopy was used for positioning and an

oblique incision through skin to fascia was made, separating abdominal muscles to expose psoas major. Direct observation to target intervertebral space was made by the insertion of a guide needle. After confirming with C-arm fluoroscopy, dilators and distractor were inserted, exposing intervertebral space. To incise the annulus fibrosus, the intervertebral disc was removed, and a bone graft bed was prepared. After trial implantation, an interbody fusion device filled with allogeneic bone particles was inserted. The C-arm confirmed the cage's position after insertion. Posterior fixation using percutaneous pedicle screws was then performed to improve segmental stability.

Automatically Calibrated PL-QCT vBMD and Radiographic Parameters Measurements

As mentioned previously, the PL-QCT system could automatically place the fat and muscle ROIs for calibration, thus ensuring calibration quality (Fig. 1). Meanwhile, the thickness of the axial section of the lumbar spine CT used in this study was 0.625 mm. Cage positions were classified as anterior and posterior based on the relationship between the vertebrae's midpoint and the cage's midpoint (Fig. 2). EP-vBMD was defined as the average vBMD of the cranial and caudal endplates based on cage position at fused levels (Fig. 3). All EP-vBMD ROIs were adjusted in parallel to the endplate. The criterion of 1.25/2.5/5-mm height ROIs with the same endplate-disk border was applied for EP-vBMD measurements. Osteoporosis is a skeletal disorder characterized by reduced bone mass, which increases fracture risk.²² The L1 and L2 average TB-vBMD was defined as the patient's QCT-BMD for osteoporosis screening based on existing standards.²³ The average of upper and lower trabecular vBMD on the fusion level was defined as TB-vBMD (Fig. 3). QCT-BMD and TB-vBMD were measured by automatically placed bone ROIs based on formal literature. Other

localized vBMD bone ROIs were placed manually. Cage position-TB-vBMD (P-TB-vBMD) was defined as the anterior or inferior trabeculae vBMD based on cage position. Sclerosis regions were excluded from all vBMD measurements. The radiographic parameters included: (i) sagittal canal diameter—the shortest distance from the posterior edge of the vertebral body to the basal line of the spinous process; (ii) lumbar lordosis—the angle between the extension line of the upper endplate of L1 and the upper endplate of S1; (3) segmental lordosis—the angle between the extension lines of the upper and lower endplates of surgical levels in the patient's preoperative lateral radiograph; and (4) foraminal height—the distance from the inferior pedicle wall of the level above to the superior pedicle wall of the level below. Demographics, EP-vBMD, QCT-BMD, TB-vBMD, position-TB-vBMD (P-TB-vBMD), and radiographic parameters were all measured in preoperative CT and X-ray images. All operations were performed by a single surgeon with at least 10 years of experience in spine surgery. Polyether ether ketone (PEEK) cages were used in single-level or multi-level XLIF with a small incision in the right recumbent position for all patients. The same endplate handling and cage placement techniques were used in all surgeries.

Cage Subsidence Assessment

Cage subsidence was determined based on the most recent postoperative sagittal plane of prone CT scans (>5 months after surgery) and lateral X-ray films are taken 5–13 months postoperatively. Based on formal research focusing on OLIF, LLIF, ALIF,^{24–26} cage subsidence is defined as >2 mm cage sinking on the adjacent endplate in the follow-up imaging including CT and X-ray scanning. Two senior spine surgeons (Mingyuan Di and Hongjin Wu) assessed cage subsidence. A consistency test was undertaken for inter-observer comparisons, the Cronbach's alpha were larger than 0.95, showing

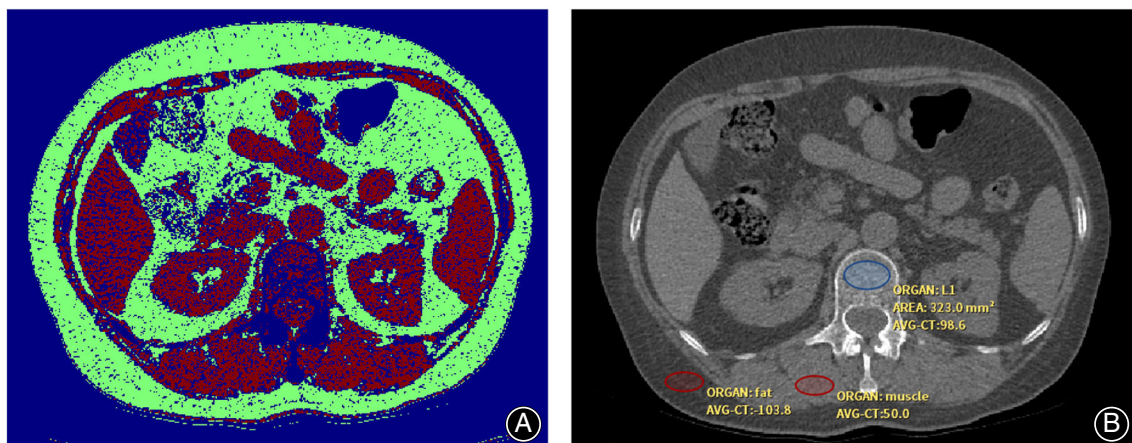


Fig. 1 Example of a CT scan processed by the PL-QCT system. (A) Green region represents fat, red region represents muscle and blue region represents others. (B) ROI position of L2 vertebral cancellous region, fat, and muscle in the cross-section of CT image. The fat and muscle ROIs were used for PL-QCT BMD calibration, they were placed automatically based on mentioned optimal algorithm.

good inter-observer reliabilities of cage subsidence assessments by the two senior spine surgeons.

Statistical Analysis

The Shapiro–Wilk test was conducted to assess the normality of continuous variables. A one-way analysis of variance (ANOVA) and Mann–Whitney test were used to evaluate differences. The Fisher exact test was used for categorical variables. Univariable and multivariable logistic regressions were conducted. In multivariable analysis, we included QCT-BMD, TB-vBMD, P-TB-vBMD, 1.25-mm EP-vBMD, and all trending ($p < 0.20$) factors in the univariable analysis as explanatory variables. Receiver operating characteristic (ROC) curve analysis was conducted for BMD, P-Tb-vBMD, and 1.25/2.5/5-mm EP-vBMD. The area under the curve (AUC) was calculated for each ROC. Statistical analysis was performed on SPSS 24.0 software (IBM, Armonk, NY, USA), $p < 0.05$ was the set significance level.

Results

Patient Demographics

A total of 78 patients were included based on the above-mentioned criteria. The mean age was 61.5 ± 7.9 years; 85.9% were female, 31 (39.7%) were overweight with a BMI of 24–28 kg/m^2 , and 22 (28.2%) were obese with a BMI > 28 kg/m^2 . The most common preoperative diagnosis was lumbar spinal stenosis (82.1%), followed by foraminal stenosis (59%), lumbar spondylolisthesis (48.7%), and degenerative scoliosis (17.9%). The mean QCT-BMD was 103.9 ± 36.9 mg/cm^3 and 28.2% of patients were classified as those with

osteoporosis (Table 1) based on their QCT-BMD results. The mean follow-up time was 16 (6–32) months. The 113 surgical levels were classified according to the definition of cage subsidence, where 45 levels (39.8%) and 68 levels (60.2%) were in the subsidence and non-subsidence groups, respectively. ANOVA for demographic information showed no statistical differences for age, gender, BMI, smoking state, previous lumbar spine surgery, number of fused levels, preoperative diagnosis, or level of fused segments (Table 2).

Vertebral Localized vBMDs Measurements

The QCT-BMD was 96.9 ± 39.4 mg/cm^3 in the subsidence group and 108.6 ± 34.6 mg/cm^3 in the non-subsidence group ($p = 0.019$). TB-vBMD was 108.8 ± 37.1 mg/cm^3 in the subsidence group and 119.9 ± 36.3 mg/cm^3 in the non-subsidence group ($p = 0.035$). P-TB-vBMD was 101.9 ± 37.3 mg/cm^3 in the subsidence group and 118.7 ± 38.2 mg/cm^3 in the non-subsidence group ($p = 0.022$). The 1.25-mm EP-vBMD was 289.2 ± 76.1 mg/cm^3 in the subsidence group and 331.0 ± 66.1 mg/cm^3 in the non-subsidence group ($p = 0.002$) (Table 3).

Relevance Analysis between Cage Subsidence and Localized vBMDs

Differential analysis of preoperative vBMD and radiographic parameters showed no statistical differences in the lumbar lordosis, segmental lordosis, sagittal canal diameter, and foraminal height. Univariate analysis showed that P-TB-vBMD (0.988 [0.977, 0.999], $p = 0.026$) and 1.25-mm EP-vBMD (0.991 [0.985, 0.997], $p = 0.004$) were more strongly associated with postoperative cage subsidence after XLIF.

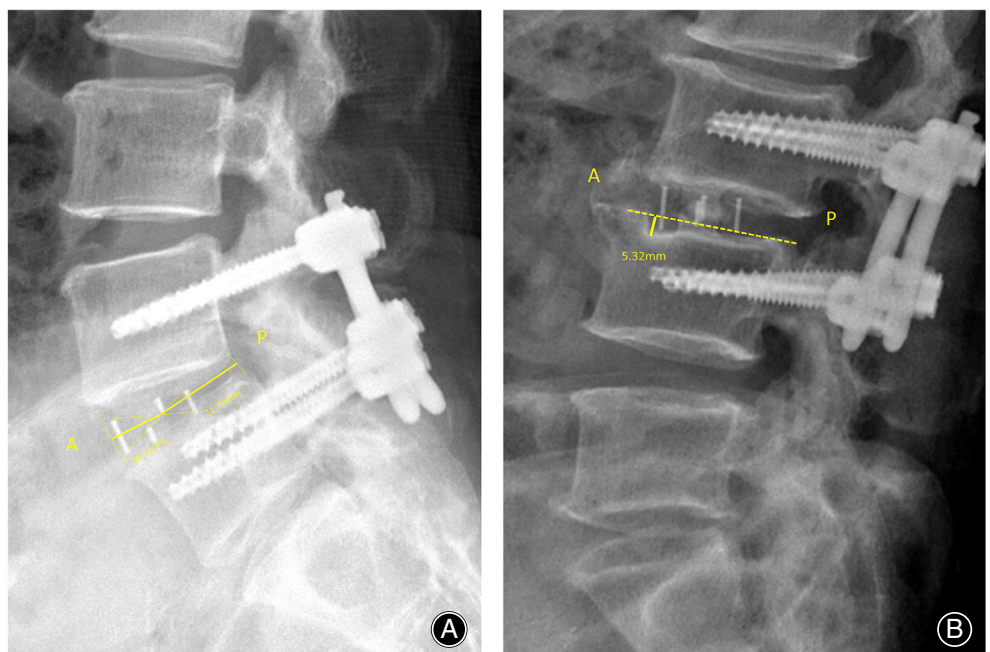


Fig. 2 Measurement of cage position AND cage subsidence. (A) Measure the distance from the midpoint of the cage to the anterior and posterior borders of the intervertebral space respectively; (B) Measure the vertical distance of the cage subsidence; For both Fig. 2A,B, yellow label A means the anterior rim of endplate and yellow label P means posterior rim of endplate.

Following univariate analysis ($p < 0.2$), BMD, P-TB-vBMD, TB-vBMD, and 1.25-mm EP-vBMD were subjected to multivariate analysis, and the results showed that low 1.25-mm EP-vBMD (0.992 [0.985, 0.999], $p = 0.029$) was an independent risk factor for cage subsidence after XLIF (Table 4). ROC curves showed that the AUC (95% CI) of BMD, P-TB-vBMD and 1.25/2.5/5 mm EP-vBMD were 0.631 (0.522–0.740), 0.640 (0.535–0.744) · 0.702 (0.599–0.805) · 0.687 (0.585–0.790), and 0.633 (0.527–0.739) respectively (Fig. 4).

Discussion

Results obtained in this study demonstrated several significant findings. First, vertebral localized vBMDs were relevantly optimal risk factors of cage subsidence, in comparison with other patients' demographics. Second, vBMDs on measured on different regions correlated with cage subsidence differently, especially for vBMDs of cancellous region and endplate region. Last but not least, EP-vBMD of the most cortex-occupied region was strongly correlated with cage subsidence and it was also an independent subsidence risk factor.

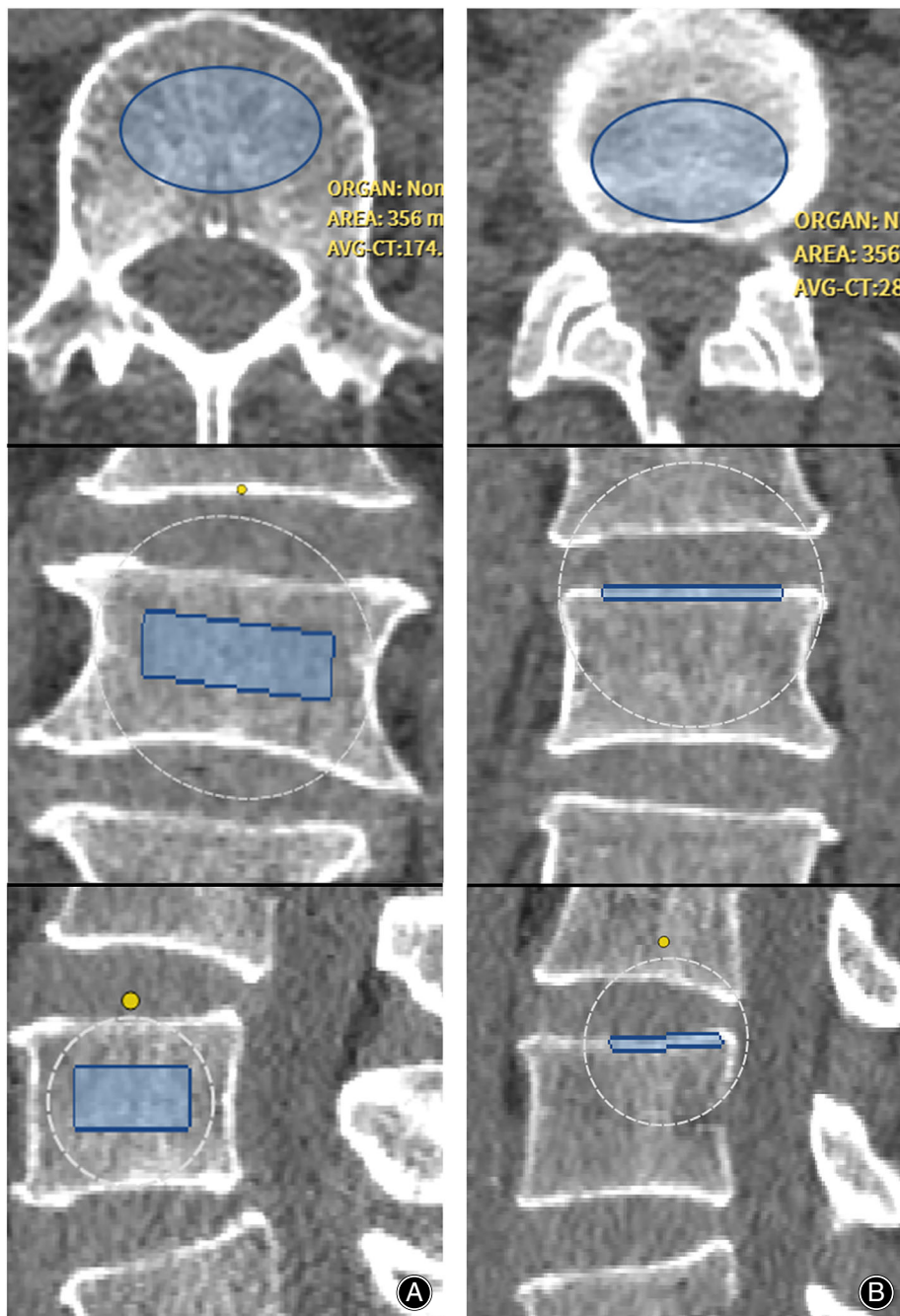


Fig. 3 vBMD measurement of trabecular bone and endplate in the axial, coronal and sagittal plane of CT image. A.L4 average trabecular bone. B.L3 posterior caudal endplate(to the disc).

TABLE 1 Patient demographics

Number of patients	78
Age (year)	
Mean [SD]	61.5 (7.9)
Sex (%)	
Female	67 (85.9)
BMI (kg/m ²)	
Mean (SD)	26.1 (4.1)
(%)	
Normal (<24 kg/m ²)	25 (32.1)
Overweight (24–28 kg/m ²)	31 (39.7)
Obese (>28 kg/m ²)	22 (28.2)
Previous lumbar surgery (%)	3 (3.8)
Preoperative diagnosis (%)	
Lumbar spinal stenosis	64 (82.1)
Foraminal stenosis	46 (59.0)
Spondylolisthesis	38 (48.7)
Adult degenerative scoliosis	14 (17.9)
Number of fused levels (%)	
1 level	53 (67.9)
2 levels	17 (21.8)
3 levels or more	8 (10.3)
QCT-BMD (mg/cm ³)	
Mean (SD)	103.9 (36.9)
>120 mg/cm ³	26 (33.3)
80–120 mg/cm ³	30 (38.5)
<80 mg/cm ³	22 (28.2)
1.25-mm EP-vBMD (mg/cm ³)	
Mean [SD]	314.4 (72.9)
Number of levels	113
Levels (%)	
L1/L2	5 (4.4)
L2/L3	15 (13.3)
L3/L4	31 (27.4)
L4/L5	62 (54.9)

Optimal Risk Factors of Cage Subsidence

We analyzed 113 levels of patients undergoing XLIF surgery, and at 45 levels subsidence was experienced. Multivariate analysis showed that low EP-vBMD was an independent risk factor for cage subsidence after XLIF. Cage subsidence is a significant complication of XLIF surgery, causing a reduction in intervertebral height and failure of indirect decompression, implying an increased risk of pain recurrence and reoperation. A meta-analysis evaluated 1362 cases of LLIF cage subsidence, of which 2.7% required reoperation.³ Our study features preoperative vertebral localized vBMD measured by automatically calibrated PL-QCT for predicting the probability of postoperative cage subsidence and personalizing the XLIF patients' surgical plans. Hounsfield Unit (HU) values, DXA, phantom-based QCT (PB-QCT), and PL-QCT have been used in formal research for BMD measurement but their accuracies vary (Table 5).

Localized vBMDs and Cage Subsidence

Xi *et al.*²⁷ showed that lower HU values on preoperative vertebral CT images were associated with cage subsidence by retrospectively analyzing the factors of cage subsidence in single-level LLIF. Wu *et al.*²⁶ showed that the HU value of the endplate is a good predictor of cage subsidence.

TABLE 2 Comparisons of demographics between subsidence group and non-subsidence group

	Non-subsidence	Subsidence	p-value
Number of levels	68	45	
Age (year)			
Mean [SD]	62.0 (8.5)	62.6 (7.9)	0.344
BMI (kg/m ²)			
Mean [SD]	26.0 (4.2)	25.8 (3.9)	0.734
Smoking state (%)	8 (11.8)	6 (13.3)	0.804
Previous lumbar surgery (%)	2 (2.9)	1 (2.2)	0.999
Operating levels (%)			
L1/L2	3 (0.4)	2 (4.4)	0.657
L2/L3	9 (13.2)	6 (13.3)	
L3/L4	16 (23.5)	15 (33.3)	
L4/L5	40 (58.8)	22 (48.9)	
Preoperative diagnosis (%)			
Lumbar spinal stenosis	58 (85.3)	36 (80.0)	0.608
Foraminal stenosis	42 (61.8)	29 (64.4)	0.844
Spondylolisthesis	25 (36.8)	21 (46.7)	0.332
Adult degenerative scoliosis	17 (25.0)	12 (26.7)	0.808
Number of fused levels (%)			
1 level	32 (47.1)	21 (46.7)	0.977
2 levels	20 (29.4)	14 (31.1)	
3 levels or more	16 (23.5)	10 (22.2)	

However, HU values for measuring BMD are controversial since measurements with different equipment and application environments can cause a bias in the grayscale values.²⁸ QCT-BMD has advanced in terms of long-term reproducibility, especially for automatically calibrated PL-QCT.¹⁴ In this study, automatically calibrated PL-QCT was utilized for vBMD measurement. It could automatically place the ROI of subcutaneous fat and paravertebral muscle to avoid operational bias. As for DXA, a previous study showed that cage subsidence after PLIF was correlated with the DXA T-score.⁶ Tempel *et al.*²⁹ showed that patients undergoing LLIF surgery had a higher risk of cage subsidence with a T-score of DXA below -1.0 . Although DXA remains the gold standard for measuring BMD, it computes areal BMD rather than volumetric BMD. Liu *et al.*¹⁴ suggested that automatic PL-QCT has higher accuracy than conventional PB-QCT and PL-QCT has good potential for future BMD assessment. Additionally, PL-QCT has the advantages of lower radiation exposure and reduced patient costs compared to conventional PB-QCT as it could be used in opportunity screening. As for its advantages in comparison with DXA, PL-QCT generates three-dimensional bone density results on cancellous region and cortical region respectively but DXA only generates two-dimensional bone density results of whole vertebral or femur segments.

Importantly, as vBMD can be measured on routine CT through the PL-QCT technique, it could be exploited as a massive-scale opportunistic bone quality screening tool. As routine CT is a necessary preoperative examination for patients requiring urgent surgery, the PL-QCT vBMD test is significant and extremely convenient. Low vBMD implies poorer bone quality and a higher likelihood of implant-related

TABLE 3 Comparisons of preoperative parameters between subsidence group and non-subsidence group

Preoperative parameter	Non-subsidence (n = 68)	Subsidence (n = 45)	p-value
Number of levels	68	45	
Lumbar lordosis (°)			
Mean (SD)	36.5 (4.9)	37.9 (2.6)	0.409
Segmental lordosis (°)			
Mean (SD)	7.4 (1.0)	7.5 (1.2)	0.619
SCD (mm)			
Mean (SD)	11.5 (0.9)	11.4 (1.0)	0.885
Foraminal height (mm)			
Mean (SD)	14.3 (1.9)	14.0 (1.9)	0.455
QCT-BMD			
Mean (SD)	108.6 (34.6)	96.9 (39.4)	0.019
Category (%)			0.816
Normal			
>120 mg/cm ³	22 (32.4)	11 (24.4)	
Osteopenia			
80–120 mg/cm ³	29 (42.6)	12 (26.7)	
Osteoporosis			
<80 mg/cm ³	25 (36.8)	14 (32.1)	
P-TB-vBMD (mg/cm ³)			
Mean (SD)	118.7 (38.2)	101.9 (37.3)	0.022
TB-vBMD (mg/cm ³)			
Mean (SD)	119.9 (36.3)	108.8 (37.1)	0.035
1.25-mm EP-vBMD (mg/cm ³)			
Mean (SD)	331.0 (66.1)	289.2 (76.1)	0.002

Abbreviation: SCD, sagittal canal diameter.

TABLE 4 Univariate analysis of risk factors for cage subsidence or cage subsidence

Factors	Odds Ratio	Lower 95% CI	Upper 95% CI	p-value
AGE	1.023	0.974	1.074	0.372
SEX(Female)	0.583	0.19	1.787	0.345
BMI	0.959	0.865	1.063	0.43
QCT-BMD	0.991	0.98	1.002	0.1
P-TB-vBMD	0.988	0.977	0.999	0.026
TB-vBMD	0.987	0.975	0.999	0.075
1.25-mm EP-vBMD	0.991	0.985	0.997	0.004

complications. vBMD assessment can help predict the risk of cage subsidence. By assessing vBMD, experienced physicians can identify patients at higher risk for cage subsidence and take appropriate preventive measures, such as choosing a different implant or considering optimal surgical planning. Simultaneously, vBMD assessment allows for individualized patient care, which can optimize surgical outcomes, reduce complications, and improve overall patient satisfaction.

Significance of Osseous Endplate on Cage Subsidence

Although the osseous endplate constitutes only a small portion of the vertebral body, it is a characteristic structure of the vertebral body. Osteoporotic vertebral compression

fractures frequently involve fractures of the osseous endplate.³⁰ Studies have shown that the average thickness of the cranial endplates (relative to the disk) of the lumbar spine is 1.03 mm, while that of the caudal endplates is 0.78 mm.¹⁹ The shape of the physiological lumbar endplates includes flat, concave, and irregular types.³¹ To cover the thickness of most osseous endplates, 1.25-mm height ROI was included in this study, and the measurements were divided into anterior, or posterior based on the cage position. Jones *et al.*¹⁶ set the thickness of the endplate measurement at 5 mm, and in fact, most of the 5 mm ROI covered was the trabecular bone. In our study, AUC results of 1.25/2.5/5 mm height EP-vBMD directly indicated that 1.25 mm height ROI which is mostly occupied by the cortex is the optimal choice for cage subsidence prediction. Such a finding clarified the influence of the osseous endplate in the XLIF cage subsidence, which is novel and innovative compared to previous studies.

The relationship between cage position and cage subsidence remains controversial. Zavras *et al.*³² showed that anterior cage placement is an independent risk factor for cage subsidence in ALIF. However, posterior cage placement is also a suggested risk factor for cage subsidence. Amorim-Barbosa *et al.*³³ suggested that posterior cage placement in PLIF and TLIF is an associated risk factor for cage subsidence. There are fewer studies on the correlation of XLIF cage position with cage subsidence. Our study measured the TB-vBMD at fusion levels. First, TB-vBMD was located in the anterior part of the vertebral body and is larger than that in the posterior part of the vertebral body. Further studies are needed to expand the sample size to explore this aspect.

The thickness of the osseous endplates differs and the cranial osseous endplate is thicker than the caudal osseous endplates.³⁴ In our study, the average cranial EP-vBMD was higher than the caudal EP-vBMD. Such consistency may prevail in a possible relationship between endplate localized thickness and endplate localized vBMD, which can be explored in further work.

Moreover, cage material and pedicle screw fixation are also important factors of cage subsidence. Seaman *et al.*³⁵ showed similar cage fusion rates for titanium and PEEK cages but increased subsidence rates for the former. In contrast, Ohiorhenuan *et al.*³⁶ concluded that titanium cages were associated with a lower subsidence incidence by univariate analysis. The subsidence rate of titanium cages is controversial, as its shape and surgical approach may be relevant. As for pedicle screw placement, Liu *et al.*³⁷ demonstrated that stand-alone XLIF produced significantly higher endplate stresses than XLIF with a posterior pedicle screw through a finite element analysis, which may also affect cage subsidence. Therefore, posterior pedicle screw fixation is suggested in patients undergoing XLIF surgery in combination with low EP-vBMD.

Strengths and Limitations

The main strength of this study was the detailed research about vertebral localized vBMDs and cage subsidence, in comparison with formal studies, this was the first time

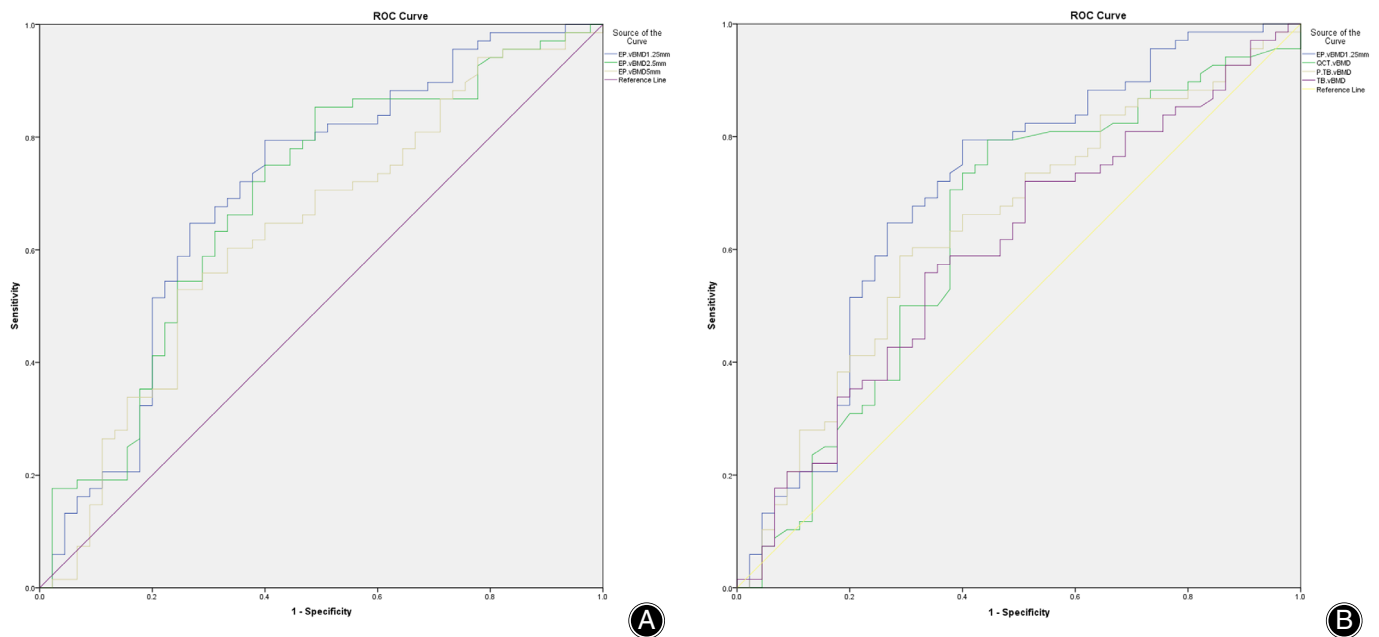


Fig. 4 ROC curves of all vBMD measurements about cage subsidence. (A) Blue curve represents 1.25-mm EP-vBMD, the green curve represents 2.5-mm EP-vBMD and the brown curve represents 5-mm EP-vBMD. (B) Blue curve represents 1.25-mm EP-vBMD, the green curve represents QCT-BMD, the brown curve presents P-TB-vBMD and the purple curve represents TB-vBMD.

TABLE 5 Multivariate analysis of risk factors for cage subsidence or cage subsidence

Factors	Odds Ratio	Lower 95% CI	Upper 95% CI	p-value
QCT-BMD	1.012	0.989	1.036	0.316
P-TB-vBMD	0.996	0.973	1.021	0.764
TB-vBMD	0.988	0.962	1.015	0.379
1.25-mm EP-vBMD	0.992	0.985	0.999	0.029

EP-vBMDs with different ROI heights were measured, which provides more information in the research field of cortical endplate and cage subsidence. The application of PL-QCT for vBMD measurements could also be a strength, as its practice in this study was a classic example of its major clinical benefit, opportunistic vBMD measurements. Without the mentioned clinical benefit, it is impossible for a retrospective vBMD study based on routine CT data.

There are some limitations to this study. Our radiographic images had a short follow-up period but Agarwal *et al.*³⁸ reviewed 623 levels of LLIF postoperatively and reported cage subsidence that occurred at a mean of 4.7 months. Some factors affecting local bone quality were not considered, such as Modic changes or changes in fat within the vertebral body; previous studies have shown that Modic changes associated with endplate sclerosis can prevent cage subsidence.³⁹ We focused on patient imaging outcomes and did not include patient-reported outcomes. We restricted our

sample to XLIF surgery cases with internal fixation systems, which may have some limitations but adding XLIF cases with stand-alone cases together would result in differences in surgical approach between the samples, and for balancing we chose to analyze XLIF surgery cases with internal fixation systems. Further work with more patient data for mentioned limitations and complete statistical analysis for all variants is needed.

Conclusion

We present a novel BMD measurement technique for more accurate cage subsidence risk evaluation. Our results showed that preoperative EP-vBMD and P-TB-vBMD were associated with postoperative cage subsidence after XLIF. Preoperative EP-vBMD was an independent risk factor for postoperative cage subsidence after XLIF; EP-vBMD measured by most cortex-occupied ROI is the optimal cage subsidence prediction parameter, which may be a potential instruction tool for cage application.

Acknowledgments

We thank Huan Qi for his contribution on software design and validation; We thank Chao Chen, Xinlong Ma, Baoshan Xu and Zhi Wang for their supervision on this study.

Conflict of Interest Statement

The authors have no conflicts of interest relevant to this article.

Ethical Statement

The authors affirm that human research participants gave informed consent for the availability of data and materials. This study was approved by Tianjin Hospital Ethics Committee.

Author contributions

Conceptualization: Yuanzhi Weng, Weijia William Lu, Qiang Yang. Methodology: Mingyuan Di, Yuanzhi Weng, Guohua Wang. Software: Huan Qi. Investigation: Mingyuan Di, Hongjin Wu. Formal Analysis: Mingyuan Di, Guohua Wang. Resources: Hanming Bian, Hongjin Wu, Yiming Dou, Shan Zhu, Chao Chen. Writing the original draft: Mingyuan Di. Writing, review and editing: Yuanzhi

Weng. Supervision: Zhi Wang, Xinlong Ma, Baoshan Xu, Weijia William Lu, Qiang Yang. Funding acquisition: Qiang Yang.

Funding Information

This study was supported by National Key R&D Program of China (2020YFC1107402), National Key R&D Program of China (2020YFC1107402), National Natural Science Foundation of China (81871782), Tianjin Science Fund for Distinguished Young Scholars (18JCQJC47900), Medical Innovation Fund for Clinical Application of National Clinical Research Center for Orthopedics, Sports Medicine & Rehabilitation (2021-NCRC-CXJJ-ZH-22).

References

- Epstein NE. Review of risks and complications of extreme lateral Interbody fusion (XLIF). *Surg Neurol Int.* 2019;10:237. https://doi.org/10.25259/SNI_559_2019
- Ozgur BM, Aryan HE, Pimenta L, Taylor WR. Extreme lateral Interbody fusion (XLIF): a novel surgical technique for anterior lumbar interbody fusion. *Spine J.* 2006;6:435–43. <https://doi.org/10.1016/j.spinee.2005.08.012>
- Macki M, Anand SK, Surapaneni A, Park P, Chang V. Subsidence rates after lateral lumbar Interbody fusion: a systematic review. *World Neurosurg.* 2018;122:599–606. <https://doi.org/10.1016/j.wneu.2018.11.121>
- Chen E, Xu J, Yang S, Zhang Q, Yi H, Liang D, et al. Cage subsidence and fusion rate in extreme lateral Interbody fusion with and without fixation. *World Neurosurg.* 2019;122:e969–77. <https://doi.org/10.1016/j.wneu.2018.10.182>
- Bocahut N, Audureau E, Poignard A, Delambre J, Queinnee S, Flouzat Lachaniette CH, et al. Incidence and impact of implant subsidence after stand-alone lateral lumbar interbody fusion. *Orthop Traumatol Surg Res.* 2018;104:405–10. <https://doi.org/10.1016/j.otsr.2017.11.018>
- Oh KW, Lee JH, Lee J-H, Lee D-Y, Shim HJ. The correlation between cage subsidence, bone mineral density, and clinical results in posterior lumbar Interbody fusion. *Clin Spine Surg.* 2017;30:E683–9. <https://doi.org/10.1097/BSD.0000000000000315>
- Park M-K, Kim K-T, Bang W-S, Cho D-C, Sung J-K, Lee Y-S, et al. Risk factors for cage migration and cage retropulsion following transforaminal lumbar interbody fusion. *Spine J.* 2019;19:437–47. <https://doi.org/10.1016/j.spinee.2018.08.007>
- Camacho PM, Petak SM, Binkley N, Diab DL, Eidey LS, Farooki A, et al. American association of clinical endocrinologists/American college of endocrinology clinical practice guidelines for the diagnosis and treatment of postmenopausal osteoporosis-2020 update. *Endocr Pract.* 2020;26:1–46. <https://doi.org/10.4158/GL-2020-0524SUPPL>
- Blake GM, Fogelman I. The role of DXA bone density scans in the diagnosis and treatment of osteoporosis. *Postgrad Med J.* 2007;83:509–17. <https://doi.org/10.1136/pgmj.2007.057505>
- Maldonado G, Intriago M, Larroude M, Aguilar G, Moreno M, Gonzalez J, et al. Common errors in dual-energy X-ray absorptiometry scans in imaging centers in Ecuador. *Arch Osteoporos.* 2020;15:6. <https://doi.org/10.1007/s11657-019-0673-3>
- Link TM, Lang TF. Axial QCT: clinical applications and new developments. *J Clin Densitom.* 2014;17:438–48. <https://doi.org/10.1016/j.jocd.2014.04.119>
- Löffler MT, Sollmann N, Mei K, Valentinitich A, Noël PB, Kirschke JS, et al. X-ray-based quantitative osteoporosis imaging at the spine. *Osteoporos Int.* 2020;31:233–50. <https://doi.org/10.1007/s00198-019-05212-2>
- Salzmann SN, Shirahata T, Yang J, Miller CO, Carlson BB, Rentenberger C, et al. Regional bone mineral density differences measured by quantitative computed tomography: does the standard clinically used L1-L2 average correlate with the entire lumbosacral spine? *Spine J.* 2019;19:695–702. <https://doi.org/10.1016/j.spinee.2018.10.007>
- Liu Z-J, Zhang C, Ma C, Qi H, Yang Z-H, Wu H-Y, et al. Automatic phantomless QCT system with high precision of BMD measurement for osteoporosis screening: technique optimisation and clinical validation. *J Orthop Translat.* 2022;33:24–30. <https://doi.org/10.1016/j.jot.2021.11.008>
- Okano I, Jones C, Salzmann SN, Reisener M, Sax OC, Rentenberger C, et al. Endplate volumetric bone mineral density measured by quantitative computed tomography as a novel predictive measure of severe cage subsidence after standalone lateral lumbar fusion. *Eur Spine J.* 2020;29:1131–40. <https://doi.org/10.1007/s00586-020-06348-0>
- Jones C, Okano I, Salzmann SN, Reisener M, Chiapparelli E, Shue J, et al. Endplate volumetric bone mineral density is a predictor for cage subsidence following lateral lumbar interbody fusion: a risk factor analysis. *Spine J.* 2021;21:1729–37. <https://doi.org/10.1016/j.spinee.2021.02.021>
- Zhao L, Xie T, Wang X, Yang Z, Pu X, Lu Y, et al. Clinical and radiological evaluation of cage subsidence following oblique lumbar interbody fusion combined with anterolateral fixation. *BMC Musculoskelet Disord.* 2022;23:214. <https://doi.org/10.1186/s12891-022-05165-4>
- Silva MJ, Wang C, Keaveny TM, Hayes WC. Direct and computed tomography thickness measurements of the human, lumbar vertebral shell and endplate. *Bone.* 1994;15:409–14.
- Wang Y, Battié MC, Boyd SK, Videman T. The osseous endplates in lumbar vertebrae: thickness, bone mineral density and their associations with age and disk degeneration. *Bone.* 2011;48:804–9. <https://doi.org/10.1016/j.bone.2010.12.005>
- Pitzen T, Schmitz B, Georg T, Barbier D, Beuter T, Steudel WI, et al. Variation of endplate thickness in the cervical spine. *Eur Spine J.* 2004;13:235–40.
- Edwards WT, Zheng Y, Ferrara LA, Yuan HA. Structural features and thickness of the vertebral cortex in the thoracolumbar spine. *Spine (Phila Pa 1976).* 2001;26:218–25.
- Akkawi I, Zmerly H. Osteoporosis: current concepts. *Joints.* 2018;6:122–7. <https://doi.org/10.1055/s-0038-1660790>
- Lewiecki EM, Gordon CM, Baim S, Leonard MB, Bishop NJ, Bianchi M-L, et al. International Society for Clinical Densitometry 2007 adult and pediatric official positions. *Bone.* 2008;43:1115–21. <https://doi.org/10.1016/j.bone.2008.08.106>
- Yao Y-C, Chou P-H, Lin H-H, Wang S-T, Liu C-L, Chang M-C. Risk factors of cage subsidence in patients received minimally invasive Transforaminal lumbar Interbody fusion. *Spine.* 2020;45:E1279–85. <https://doi.org/10.1097/brs.0000000000000357>
- Parisien A, Wai EK, ElSayed MSA, Frei H. Subsidence of spinal fusion cages: a systematic review. *Int J Spine Surg.* 2022;16:1103–18. <https://doi.org/10.14444/8363>
- Wu H, Cheung JPY, Zhang T, Shan Z, Zhang X, Liu J, et al. The role of Hounsfield unit in intraoperative endplate violation and delayed cage subsidence with oblique lateral Interbody fusion. *Global Spine J.* 2021;13:21925682211052516. <https://doi.org/10.1177/21925682211052516>
- Xi Z, Mummaneni PV, Wang M, Ruan H, Burch S, Deviren V, et al. The association between lower Hounsfield units on computed tomography and cage subsidence after lateral lumbar interbody fusion. *Neurosurg Focus.* 2020;49:E8. <https://doi.org/10.3171/2020.5.FOCUS20169>
- Engelke K, Lang T, Khosla S, Qin L, Zysset P, Leslie WD, et al. Clinical use of quantitative computed tomography-based advanced techniques in the Management of Osteoporosis in adults: the 2015 ISCD official positions—part III. *J Clin Densitom.* 2015;18:393–407. <https://doi.org/10.1016/j.jocd.2015.06.010>
- Tempel ZJ, Gandhoke GS, Okonkwo DO, Kanter AS. Impaired bone mineral density as a predictor of graft subsidence following minimally invasive transpsoas lateral lumbar interbody fusion. *Eur Spine J.* 2015;24(Suppl 3):414–9. <https://doi.org/10.1007/s00586-015-3844-y>
- Tarantino U, Celi M, Feola M, Liuni FM, Resmini G, Iolascon G. A new antiresorptive approach to the treatment of fragility fractures: long-term efficacy and safety of denosumab. *Aging Clin Exp Res.* 2013;25(Suppl 1):S65–9. <https://doi.org/10.1007/s40520-013-0082-1>
- Rodríguez AG, Rodríguez-Soto AE, Burghardt AJ, Berven S, Majumdar S, Lotz JC. Morphology of the human vertebral endplate. *J Orthop Res.* 2012;30:280–7. <https://doi.org/10.1002/jor.21513>

- 32.** Zavras AG, Federico V, Nolte MT, Butler AJ, Dandu N, Munim M, et al. Risk factors for subsidence following anterior lumbar Interbody fusion. *Global Spine J.* 2022;20:21925682221103588. <https://doi.org/10.1177/21925682221103588>
- 33.** Amorim-Barbosa T, Pereira C, Catelas D, Rodrigues C, Costa P, Rodrigues-Pinto R, et al. Risk factors for cage subsidence and clinical outcomes after transforaminal and posterior lumbar interbody fusion. *Eur J Orthop Surg Traumatol.* 2021;32:1–9. <https://doi.org/10.1007/s00590-021-03103-z>
- 34.** Yeni YN, Dix MR, Xiao A, Oravec DJ, Flynn MJ. Measuring the thickness of vertebral endplate and shell using digital tomosynthesis. *Bone.* 2022;157:116341. <https://doi.org/10.1016/j.bone.2022.116341>
- 35.** Seaman S, Kerezoudis P, Bydon M, Torner JC, Hitchon PW. Titanium vs. polyetheretherketone (PEEK) interbody fusion: meta-analysis and review of the literature. *J Clin Neurosci.* 2017;44:23–9. <https://doi.org/10.1016/j.jocn.2017.06.062>
- 36.** Ohiorhenuan IE, Walker CT, Zhou JJ, Godzik J, Sagar S, Farber SH, et al. Predictors of subsidence after lateral lumbar interbody fusion. *J Neurosurg Spine.* 2022;37:1–5. <https://doi.org/10.3171/2022.1.SPINE201893>
- 37.** Liu X, Ma J, Park P, Huang X, Xie N, Ye X. Biomechanical comparison of multilevel lateral interbody fusion with and without supplementary instrumentation: a three-dimensional finite element study. *BMC Musculoskelet Disord.* 2017;18:63. <https://doi.org/10.1186/s12891-017-1387-6>
- 38.** Agarwal N, White MD, Zhang X, Alan N, Ozpinar A, Salvetti DJ, et al. Impact of endplate-implant area mismatch on rates and grades of subsidence following stand-alone lateral lumbar interbody fusion: an analysis of 623 levels. *J Neurosurg Spine.* 2020;33:1–5. <https://doi.org/10.3171/2020.1.SPINE19776>
- 39.** Liu J, Ding W, Yang D, Wu H, Hao L, Hu Z, et al. Modic changes (MCs) associated with endplate sclerosis can prevent cage subsidence in oblique lumbar Interbody fusion (OLIF) stand-alone. *World Neurosurg.* 2020;138:e160–8. <https://doi.org/10.1016/j.wneu.2020.02.047>